

Effect of temperature on the dynamics and geometry of reactive-wetting interfaces around room temperature

Meital Harel and Haim Taitelbaum

Department of Physics, Bar-Ilan University, Ramat-Gan 52900, Israel

(Received 12 July 2017; published 1 December 2017)

The temperature effect on the dynamics and geometry of a mercury droplet ($\sim 150 \mu\text{m}$) spreading on a silver substrate (4000 \AA) was studied. The system temperature was controlled by a heating stage in the temperature range of $-15^\circ\text{C} < T < 25^\circ\text{C}$, and the spreading process was monitored using an optical microscope. We studied the wetting dynamics (droplet radius and velocity) as a function of temperature. We found that for all studied temperatures, the spreading radius $R(t)$ grows linearly with time, with a velocity value depending on temperature. We also studied the temperature effect on the kinetic roughening properties of the advancing interface (growth (β) and roughness (α) exponents). Our results show that the growth exponent increases with temperature while the roughness exponent is relatively constant. In addition, we obtained the system's activation energy at this temperature range.

DOI: [10.1103/PhysRevE.96.062801](https://doi.org/10.1103/PhysRevE.96.062801)

I. INTRODUCTION

This research deals with the dynamics and geometry of a mercury droplet spreading on and reacting with a silver substrate around room temperature. The specific reaction product is useful for the medical field, especially in dentistry [1]. We studied the interface between the two materials and the droplet dynamics as a function of temperature in the range of $-15^\circ\text{C} < T < 25^\circ\text{C}$. Since at this temperature range the mercury is liquid and the silver is solid, one can investigate this system's reactive-wetting characteristics at relatively low temperatures, in contrast to most reactive-wetting processes which take place only at very high temperatures. Owing to the reaction, other possible temperature-affected processes such as evaporation are negligible.

According to the mercury-silver binary phase diagram [2], the possible phases that co-exist at this temperature range are solid solution (close to the interface), ε -phase (Ag_4Hg_3), and γ -phase (Ag_3Hg_4) close to the droplet center, depending on the Hg concentration. Temperature variations are expected to affect the surface tension, the reaction rate and the mercury's viscosity of all phases. Therefore, the temperature variation might shed light on the mechanisms which control the process at the different time and space ranges.

The main influence of temperature on chemical reactions is manifested through the chemical reaction rate. In order for particles to react, a certain energy barrier must be overcome. This minimal energy is termed E_a , the activation energy. When the temperature rises, more particles have the required energy and the reaction rate increases. The dependence of the reaction rate, k , on the temperature, T , is described by the empirical Arrhenius equation [3]:

$$k = A \exp(-E_a/RT). \quad (1)$$

This equation is valid only if A and E_a do not change with temperature, a reasonable assumption when the temperature range is not too wide. The constant A , the frequency factor, is related to the collision frequency and R is the gas constant ($8.314 \text{ J mol}^{-1} \text{ K}^{-1}$). This equation combines the collision rate with the Boltzman factor that represents the fractional part of the collisions with enough kinetic energy. The result is

the rate of successful collisions that produce reactions. Lee *et al.* [4] measured the average diffusion coefficient of the gamma phase of mercury-silver at the temperature range of $40^\circ\text{C} < T < 115^\circ\text{C}$, and found a temperature dependence in Arrhenius form,

$$D_{av}[\text{cm}^2/\text{s}] = 3.181 \times 10^{-5} \exp(-32539[\text{J/mol}]/RT), \quad (2)$$

which implies an activation energy of 32539 J/mol at this range.

Another characteristic which is directly affected by temperature is the material's viscosity [5]. Mercury's viscosity decreases when temperature increases, as shown in Fig. 1, following Ref. [6]. At the temperature range of $-20^\circ\text{C} < T < 30^\circ\text{C}$, mercury's viscosity decreases with temperature between the values of 1.855 mPas s (at -20°C) to 1.499 mPas s (at 30°C). This range covers room temperature.

A. Wetting and reactive-wetting

Many researches [7–9] theoretically and experimentally study wetting systems (without chemical reactions) on homogeneous and heterogeneous surfaces. Many studies find the time evolution of the droplet radius $R(t)$ and the wetting angle $\theta(t)$. Tanner [10] assumed that the spreading process is a competition between capillary forces that drive the liquid to wet the surface, and the liquid viscosity which attenuates the wetting process, while gravity is negligible. This assumption resulted in Tanner's law, $R(t) \sim t^{1/10}$ and $\theta(t) \sim t^{-3/10}$ [10].

In reactive-wetting systems, the droplet dynamics are different from the dynamics of classical wetting systems, with a phase formed as a consequence of interfacial reactions [11]. In several reactive-wetting systems [12,13], the spreading process was found to be characterized by a linear dependence of the droplet radius on time, $R(t) \sim t$, very different from Tanner's law.

In this paper we focus on a reactive-wetting system, first investigated by Be'er and coworkers [14–22] where mercury droplets ($150 \mu\text{m}$ diameter) were deposited on silver films of various thicknesses ($2000\text{--}6000 \text{ \AA}$) at room temperature (Fig. 2). Two stages were found in the spreading process [18,19], the "bulk propagation" regime and the fast flow

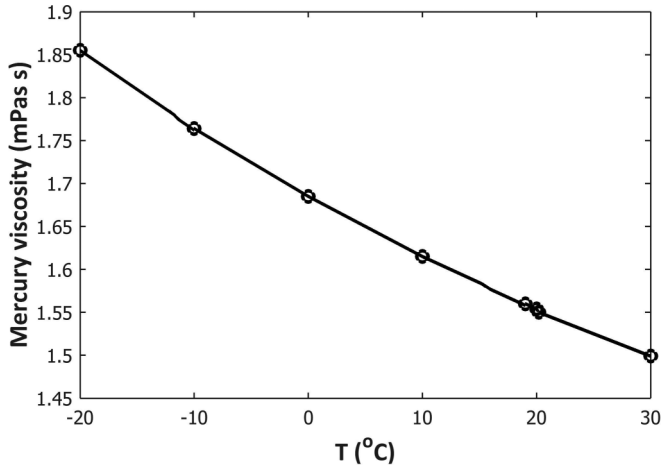


FIG. 1. Mercury viscosity versus temperature (after Ref. [6]).

regime. At the initial stage, the droplet starts to spread circularly and symmetrically. The droplet radius was found to grow linearly, $R(t) \sim t$ (as found in Refs. [12,13]), with a constant velocity of about 2–4.5 $\mu\text{m/s}$ in various experimental conditions in room temperature [14,18,19]. The contact angle $\theta(t)$ decreases continuously up to time t_d , when the mercury crosses the entire silver layer and touches the underlying glass, which its low surface energy is a key factor in such processes [18,19]. The time t_d was shown to be proportional to the square of the silver thickness, suggesting a diffusive motion inside the film [18,19]. The second stage, the “fast flow” regime, starts at t_d , when a new and thin front (500 Å) flows ahead of the contact line with a much higher velocity than the bulk front (about 1–2 orders of magnitude). A sudden step in the decreasing trend of $\theta(t)$ also occurs at this time t_d . The fast-flow dynamics gives rise to the formation of a reaction band which starts within the fast-flow time regime and grows with the average velocity of the bulk propagation regime [18]. The kinetic roughening of this reaction band is discussed in Sec. IB.

Back to wetting without chemical reaction, the effect of temperature on spreading droplets was studied by Davidovitch *et al.* [23] in the context of thermal fluctuation influences on the shape and rate of spreading droplets with specific viscosity on a solid surface. They showed numerically and analytically that the average radius of these droplets increases faster than for droplets without thermal fluctuations: $R(t) \sim t^{1/6}$ compared with $R(t) \sim t^{1/10}$ (Tanner’s law).

B. Kinetic roughening of interfaces

In the aforementioned reaction band, a dynamic interface is created between the liquid mercury and the silver substrate

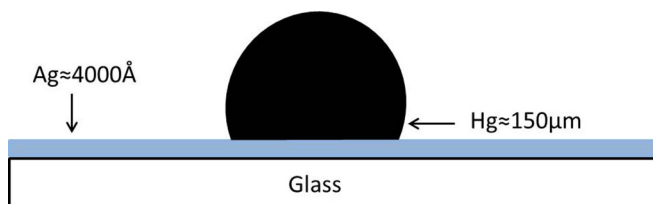


FIG. 2. Schematic description of a mercury droplet spreading on a silver substrate.

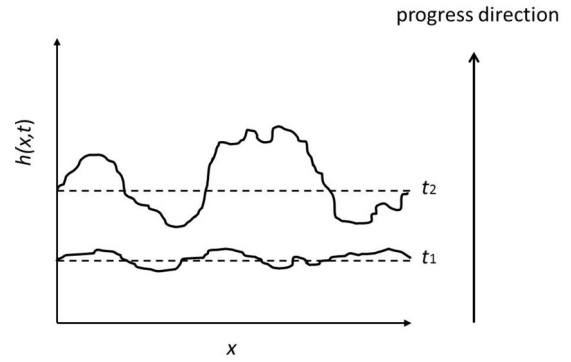


FIG. 3. Interfaces described by $h(x,t)$ for two typical times, $t_2 > t_1$.

[18]. Such an interface can be top-view described by a function $h(x,t)$, for the “height” of the interface at position x at time t (Fig. 3).

We then define the fluctuation function W for the interface width (Fig. 4),

$$W^2(L,t) = \langle h(x,t)^2 \rangle - \langle h(x,t) \rangle^2, \tag{3}$$

where the average is over all x values between 0 or the minimal length scale in the system (e.g., lattice unit) up to half of the system size $L_0/2$.

Family-Vicsek [24,25] assumed that the width W behavior can be described by the scaling relation:

$$W(L,t) \sim L^\alpha f\left(\frac{t}{L^{\alpha/\beta}}\right), \tag{4}$$

with α and β being the roughness and growth exponents, respectively, and $f(x)$ is a scaling function that behaves asymptotically as

$$f(x) \approx \begin{cases} x^\beta, & x \ll 1 \\ \text{const}, & x \gg 1 \end{cases} \tag{5}$$

This implies that W behaves differently for two time regimes [26]:

$$W(L,t) \approx \begin{cases} t^\beta, & t \ll t_0 \\ L^\alpha, & t \gg t_0 \end{cases} \tag{6}$$

At the beginning of the process, the interface width increases as t^β , according to the growth exponent β . This continues up to time $t_0 \approx L_0^{\alpha/\beta}$, when the interface width saturates. At this regime, the width behaves as L^α and one can extract the interface roughness defined by the roughness exponent α , which is related to the interface’s autocorrelation. When $\alpha > 0.5$, there is a strong correlation between nearby interface points which tend to progress in a similar manner,

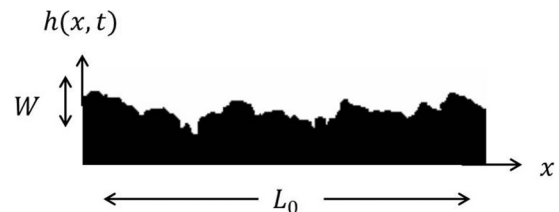


FIG. 4. A typical interface at a specific time.

TABLE I. The effect of temperature on scaling exponents of advancing interfaces in different systems.

System	Ref.	$\beta(T)$	$\alpha(T)$
Particles perform SD on a surface	[27–29]	Decreasing	Decreasing
SD contribution for evaporated gold surfaces	[30]	–	No change
Growth process of CdTe thin films	[31]	Increasing	–

with $\alpha \rightarrow 1$ for a smooth interface. $\alpha = 0.5$ describes a lack of correlation (random walk), where every point on the interface moves randomly and independently on the surroundings. $\alpha < 0.5$ describes anticorrelations between the points.

At room temperature, Efraim *et al.* [20,22] investigated the reactive-wetting process of a $150 \mu\text{m}$ Hg droplet spreading on a 4000 \AA thick Ag substrate. The growth exponent β was found to be $\beta = 0.67 \pm 0.06$ and the roughness exponent $\alpha = 0.83 \pm 0.00$ [21].

Several works study the temperature effect on kinetic roughening properties of advancing interfaces. Das Sarma *et al.* [27–29] studied a system where particles were deposited on a surface and performed surface diffusion. At relatively low temperatures ($T = 400 \text{ K}$), the diffusion is negligible, meaning that the atoms “stick” to the landing site on the interface, and $\beta = 1/2$. At intermediate temperatures ($T \sim 500 \text{ K}$), the diffusion process becomes relevant, and the growth exponent decreases to $\beta = 3/8$. At high temperatures ($T \sim 700 \text{ K}$), the diffusion length becomes higher than the system’s size, and the atoms seek a better place with lower energy. As a result, the interface becomes smoother and β decreases with temperature. Regarding α , at low temperatures the interface does not saturate at long times; therefore, the roughness exponent becomes a nonmeasurable parameter. At other temperatures, α decreases with temperature.

Zubimendi *et al.* [30] checked the surface diffusion (SD) contribution to the roughness of gold surfaces that were created by evaporation. This influence was tested during changing the temperature of surface growth or during the addition of chemical solutions. The roughness exponent did not change (~ 0.9) due to temperature variations (298 K compared to 673 K).

Ferreira *et al.* [31] studied the influence of the temperature on the growth exponent of CdTe thin films at the temperature range of $150^\circ\text{C} < T < 300^\circ\text{C}$ and found that the growth exponent increases exponentially from 0.14 to 0.62.

The various effects of temperature in these systems are summarized in Table I. One can see that the temperature effect on the growth and roughness exponents depends on

the definition of the interface at any given system. Hence we would like to explore the temperature influence on the kinetic roughening exponents of the reactive-wetting system around room temperature.

II. RESEARCH METHODOLOGY

The experimental setup is shown on Fig. 5. The spreading process of Hg on the Ag surface was monitored using an optical microscope equipped with differential interference contrast (DIC) system, and an analog colored 3CCD SONY video camera (model DXC-930P) with a resolution of 525 lines and 700 columns. The noise was significantly smaller than the real signal (signal to noise ratio is 56dB) and the video movie resolution was 25 frames per second. The movie was transferred to the computer using a frame grabber (AV/DV DELLUX, PINNACLE) and the editing software used was Studio 9. The experiment was recorded *in situ*.

To control the system’s temperature, we used a heating stage (LINKAM), with a temperature range of $-25^\circ\text{C} < T < 99^\circ\text{C}$ ($\pm 0.1^\circ\text{C}$). To prevent water vapor from condensing as drops on the surface, the substrate was surrounded by a perspex box. The box had a steady flow of nitrogen vapors from a dry nitrogen balloon so that the nitrogen vapors replaced the water vapors. Water channels were connected to the heating stage motor to prevent it from overheating. The silver substrate was placed on this stage for five minutes so that the entire surface was at the desired temperature. We then deposited a mercury droplet ($150 \mu\text{m}$ diameter) on the silver substrate (4000 \AA thickness) and the process started. The experiments were performed at the temperature range of $-15^\circ\text{C} < T < 25^\circ\text{C}$, since at higher temperatures the emission of poison gases is accelerated, and at lower temperatures it is difficult

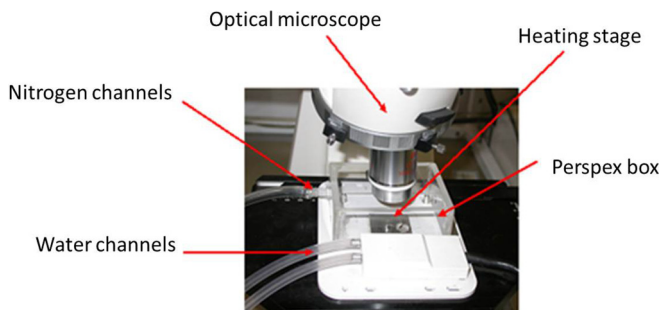
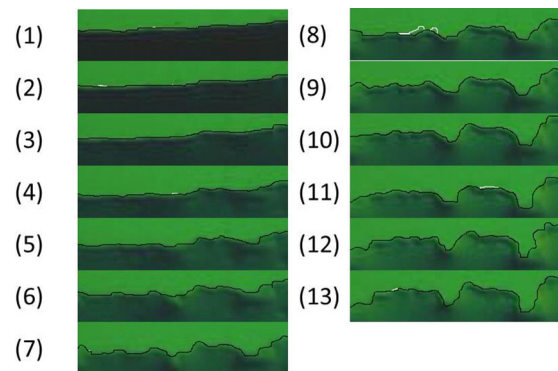


FIG. 5. The experimental setup.

FIG. 6. Pictures 1–13. Successive snapshots of the growing interface for a single experiment at $T = -15^\circ\text{C}$. The time interval between snapshots is 2 s. The scale of each snapshot is $25 \times 6.179 \mu\text{m}$.

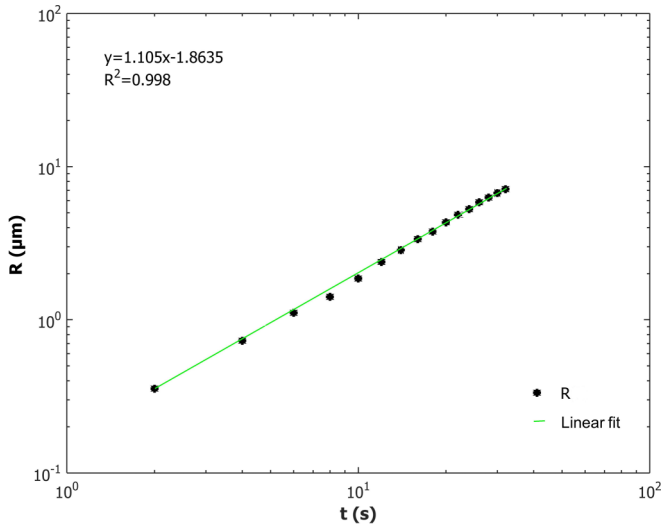


FIG. 7. $R(t)$ (log-log scale), $T = -15^\circ\text{C}$, single experiment.

to prevent water condensation. Every experiment at a given temperature was repeated 5–7 times.

Figure 6 shows a series of snapshots of the growing interface, taken for one of the experiments at $T = -15^\circ\text{C}$. The initial snapshot was taken at time $t = 6$ s and the last one at $t = 30$ s, all at equal time intervals of 2 s. The interface length is 300 pixels = $25\ \mu\text{m}$.

III. RESULTS

A. Droplet spreading velocity

In our experiments, after the interface was determined (see Fig. 6), the average location of the interface at each time could be found, and the averaged interface velocity could be calculated. Figure 7 shows the dependence of the droplet radius on time for a single experiment at $T = -15^\circ\text{C}$. The slope is 1.105, slightly above the expected linearity. The velocity for this experiment is $0.460\ \mu\text{m/s}$. The averaged velocity for this temperature is $0.225 \pm 0.074\ \mu\text{m/s}$.

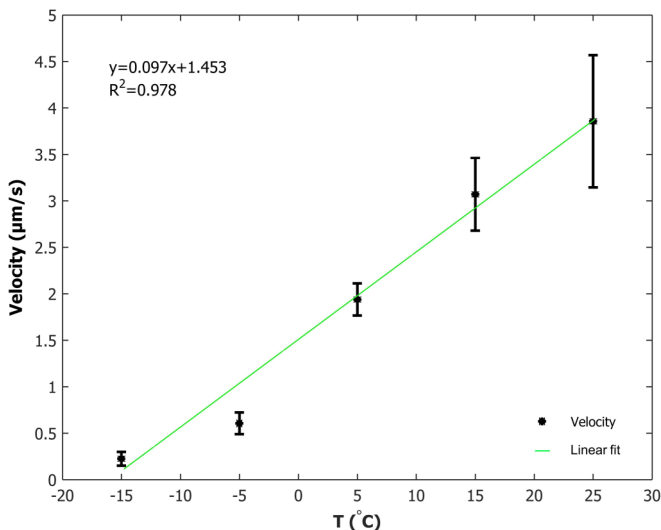


FIG. 8. The droplet spreading velocity vs. temperature.

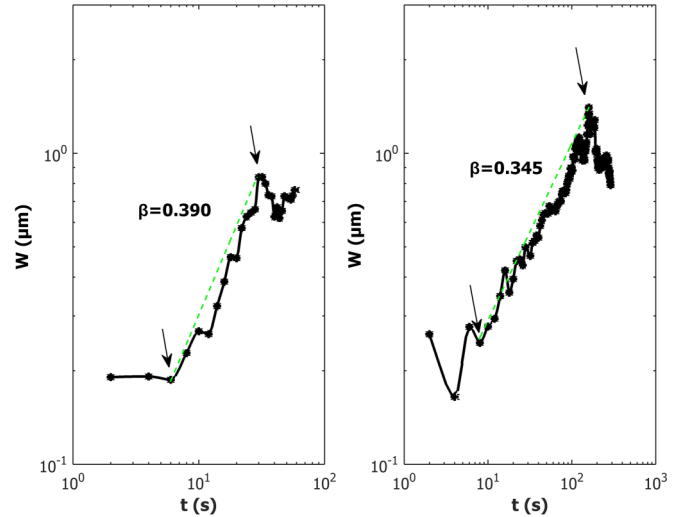


FIG. 9. $W(t)$ (log-log scale), $T = -15^\circ\text{C}$, single experiments. The arrows indicate the growth regime. The growth exponent β is calculated by a linear fit of the growth regime.

Applying the same methodology for all other temperatures, we found that the dependence of R on t is very close to linearity, and the resulting velocity is constant. The results for the droplet average velocity are shown in Fig. 8 and Table II, along with other results which will be further discussed. The conclusion is that the dependence of the droplet radius on time is qualitatively similar to other reactive-wetting systems [12,13], $R(t) \sim t$. This qualitative behavior does not depend on the temperature. However, the velocity values at each temperature grow linearly with temperature.

B. Kinetic roughening exponents

1. Growth exponent β

The interface width was calculated according to the scheme described above [Eq. (3)], for the interface segment (“window”) of $L_0/2$ (150 pixels = $12.5\ \mu\text{m}$), at fixed time intervals for each temperature. In Fig. 9 we show the results for the interface width as a function of time, $W(t)$, for two single experiments ($T = -15^\circ\text{C}$). The growth regime where β is defined is marked with arrows. The preceding region is the bulk spreading regime [18], when the mercury droplet perimeter does not develop any roughness yet. Later, the interface width grows, and then it saturates. To properly calculate the growth exponent β , a new time axis should be set corresponding to the start of growth. The growth exponent, which is the slope of the width versus the shifted time in log-log scale, was found to be, e.g., 0.390 in one experiment, and 0.345 in another, both shown in Fig. 9.

Averaging over the seven experiments performed for $T = -15^\circ\text{C}$, we found β to be 0.324 ± 0.068 . In a similar fashion, we found the averaged β for each temperature. The results are summarized in Table II and Fig. 10.

Our results clearly indicate that in the studied temperature range β increases with temperature. The result at room temperature as shown in Fig. 10, coincides with the result of earlier works showing $\beta = 0.67 \pm 0.06$ [20,22]. In some sense it is quite intuitive that β , which describes the system’s

TABLE II. Results for the average velocity, β , and α at various temperatures.

T (°C)	No. of experiments	Average velocity [$\mu\text{m/s}$]	Growth exponent β	Roughness exponent α
25	6	3.856 ± 0.711	0.655 ± 0.155	0.793 ± 0.013
15	5	3.070 ± 0.389	0.674 ± 0.135	0.817 ± 0.011
5	7	1.939 ± 0.173	0.586 ± 0.118	0.801 ± 0.012
-5	7	0.606 ± 0.117	0.444 ± 0.071	0.843 ± 0.019
-15	7	0.225 ± 0.074	0.324 ± 0.068	0.843 ± 0.016

dynamical development with time, would be directly affected by the system's temperature. However, as was described in the introduction, there could have been other possibilities as well.

Our result agrees qualitatively with the results of Ferreira *et al.* [31] regarding the increase of β with temperature, as well as with the results of Davidovitch *et al.* [23], that the droplet's expansion with thermal noise is faster. Das Sarma *et al.* [27–29], in a SD system, found that β decreased with temperature. The reason might be that in an SD system, diffusion becomes stronger when temperature increases and interface width grows slower, while in the reactive-wetting system, the reaction rate increases with temperature, mercury viscosity decreases with temperature, and the interface width increases with temperature.

2. Roughness exponent α

At late times ($t = 128$ s), the interface width saturates and the roughness exponent α was calculated. The interface width was calculated according to the scheme described above [Eq. (3)], for interface segments (“windows”) between one pixel ($\sim 0.083 \mu\text{m}$) and $L_0/2$ (150 pixels = $12.5 \mu\text{m}$), at the last snapshot of the experiment (see Fig. 11) where the roughness exponent is defined. In Fig. 12, we plotted the interface width versus the window length L in a log-log plot for a single experiment ($T = -15^\circ\text{C}$), with α as the slope.

Figure 12 exhibits the crossover phenomenon in the behavior of α [25]. For short distances, α is around 0.8 (representing strong correlation), while for distances beyond

the lateral correlation length [17] it crosses over to around 0.5 (representing randomness). The lateral correlation length for this temperature was found to be $9.58 \mu\text{m}$ (115 pixels). Averaging over all experiments at this temperature, we found the averaged α (prior to the crossover) to be 0.843 ± 0.016 . Using this method, we found the averaged α for each temperature. The results are summarized in Table II.

The roughness exponent at the temperature range of $-15^\circ\text{C} < T < 25^\circ\text{C}$ is between 0.793 and 0.843, i.e., relatively constant with temperature. It does not depend on the spreading dynamics as it is calculated based on data at the end of the process. It is interesting to note that in this very system [32], it was also found that α does not depend on the texture of the substrate's roughness, and its value is relatively constant. This means that α is material dependent only [21,32]. This is similar to the findings of Zubimendi *et al.* [30], who found that α is constant with temperature in thin gold films growth. The result for the MBE model [28], where particles perform SD, that α decreases with temperature, was obtained over a large temperature range ($500 \text{ K} < T < 660 \text{ K}$). In our system, the range is much smaller ($-15^\circ\text{C} < T < 25^\circ\text{C}$).

C. Activation energy

The Arrhenius equation [Eq. (1)] can be rewritten in terms of the velocity as

$$V = A \exp(-E_a/RT), \quad (7)$$

with the explicit gas constant R , we have

$$\ln V = \ln A + (10^4/T)(-E_a/8.31 \times 10^4). \quad (8)$$

Once the averaged interface velocity for each temperature is known, the slope of $\ln V$ versus $10^4/T$ indicates the activation energy of the system [3]. This is shown in Fig. 13 for our mercury-silver system. The comparison between the slope value (-0.567) to $(-E_a/8.31 \times 10^4)$ yields the activation energy for this system, 47175 J mol^{-1} .

Lee *et al.* [4] found that the activation energy of the gamma phase of mercury-silver at the temperature range of

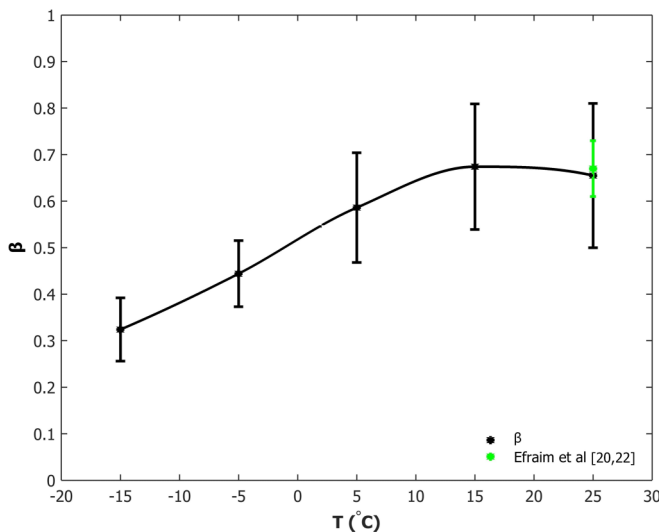


FIG. 10. β values vs. temperature. β increases with temperature. The result at room temperature coincides with Efraim *et al.* [20,22].



FIG. 11. The last snapshot of an experiment, $T = -15^\circ\text{C}$. Picture scale is $25 \times 12.075 \mu\text{m}$.

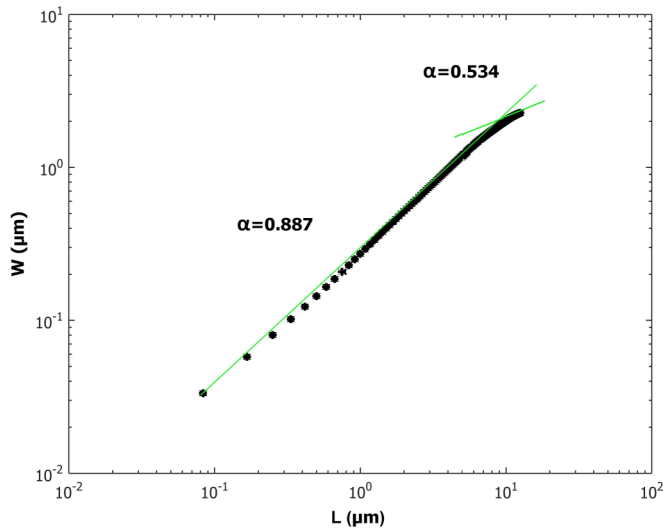


FIG. 12. $W(L)$ (log-log scale), $T = -15^\circ\text{C}$, single experiment.

$40^\circ\text{C} < T < 115^\circ\text{C}$ is 32539 J mol^{-1} . The order of magnitude of these two results is similar. Arrhenius equation is based on the assumption that the activation energy E_a and the frequency factor A do not change within the relevant temperature range. This assumption is more likely to hold in our narrower temperature range (40°C rather than 75°C). Hence we believe that our results are more accurate, definitely around room temperature. Yet, the slight discrepancy can be also explained on the basis of the specific gamma phase of Lee *et al.* [4], which is only one of the coexisting phases in our system.

IV. SUMMARY

The effect of temperature on the dynamics and geometry of a mercury droplet ($\sim 150\ \mu\text{m}$) spreading on a silver substrate ($4000\ \text{\AA}$) was studied at around room temperature, in the range $-15^\circ\text{C} < T < 25^\circ\text{C}$. The spreading process is linear, $R(t) \sim t$, for all temperatures, meaning that the reactive-wetting

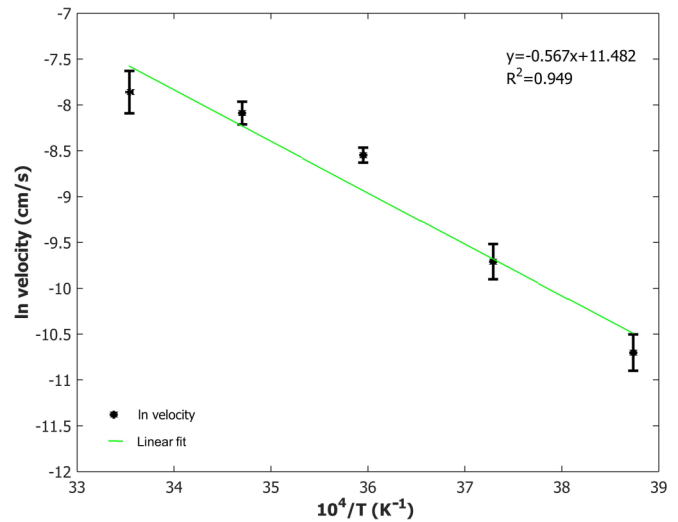


FIG. 13. The activation energy in the mercury-silver system around room temperature.

typical behavior is temperature independent. The temperature influences the proportionality constant, i.e., the velocity value, which was found to increase linearly with temperature. Regarding the interface kinetic roughening, the growth exponent β was found to increase with temperature. The roughness exponent α seems to be constant and does not depend on the spreading dynamics. For all studied temperatures, α was found to be around 0.8. This result contributes to the richness of behaviors observed for these scaling exponents under varying temperatures in various systems. The activation energy in the studied temperature range was found to be 47175 J mol^{-1} .

In summary, our results show the temperature's role in the behavior of reactive-wetting systems, not only in very high temperatures, but also in much lower temperatures, around room temperature.

ACKNOWLEDGMENT

We thank Avraham Be'er for his help in the experiment and for his constructive comments.

-
- [1] R. Nowakowski, J. Pielaszek, and R. Dus, *Appl. Surf. Sci.* **199**, 40 (2002).
 - [2] M. Hansen, *Constitution of Binary Alloys*, 2nd ed. (Macgraw-Hill, New York, 1958).
 - [3] P. Atkins and J. de Paula, *ATKINS' Physical Chemistry*, 7th ed. (Oxford University Press, Oxford, 1998).
 - [4] K. H. Lee, M. C. Shin, and J. Y. Lee, *J. Mater. Sci.* **21**, 2430 (1986).
 - [5] W. J. Moore, *Physical Chemistry*, 1st ed. (Prentice-Hall, Englewood Cliffs, NJ, 1962).
 - [6] R. C. Weast, *Handbook of Chemistry and Physics*, 70th ed. (CRC Press, Boca Raton, FL, 1989–1990).
 - [7] P. G. de Gennes, *Rev. Mod. Phys.* **57**, 827 (1985).
 - [8] L. Leger and J. F. Joanny, *Rep. Prog. Phys.* **55**, 431 (1992).
 - [9] D. Bonn, J. Eggers, J. Indekeu, J. Meunier, and E. Rolley, *Rev. Mod. Phys.* **81**, 739 (2009).
 - [10] A. Oron, S. H. Davis, and S. G. Bankoff, *Rev. Mod. Phys.* **69**, 931 (1997).
 - [11] S. Avraham and W. D. Kaplan, *J. Mater. Sci.* **40**, 1093 (2005).
 - [12] K. Landry and N. Eustathopoulos, *Acta Mater.* **44**, 3923 (1996).
 - [13] N. Eustathopoulos, *Acta Mater.* **46**, 2319 (1998).
 - [14] A. Be'er, Y. Lereah, and H. Taitelbaum, *Physica A* **285**, 156 (2000).
 - [15] A. Be'er, Y. Lereah, I. Hecht, and H. Taitelbaum, *Physica A* **302**, 297 (2001).
 - [16] A. Be'er, Y. Lereah, A. Frydman, and H. Taitelbaum, *Physica A* **314**, 325 (2002).
 - [17] A. Be'er, I. Hecht, and H. Taitelbaum, *Phys. Rev. E* **72**, 031606 (2005).

- [18] A. Be'er, Y. Lereah, A. Frydman, and H. Taitelbaum, *Phys. Rev. E* **75**, 051601 (2007).
- [19] A. Be'er, Y. Lereah, and H. Taitelbaum, *Mater. Sci. Eng. A* **495**, 102 (2008).
- [20] Y. Efraim and H. Taitelbaum, *Cent. Eur. J. Phys.* **7**, 503 (2009).
- [21] L. Yin, B. T. Murray, S. Su, Y. Sun, Y. Efraim, H. Taitelbaum, and T. J. Singler, *J. Phys.: Condens. Matter* **21**, 464130 (2009).
- [22] Y. Efraim and H. Taitelbaum, *Phys. Rev. E* **84**, 050602(R) (2011).
- [23] B. Davidovitch, E. Moro, and H. A. Stone, *Phys. Rev. Lett.* **95**, 244505 (2005).
- [24] F. Family and T. Vicsek, *J. Phys. A* **18**, L75 (1985).
- [25] T. Vicsek, *Fractal Growth Phenomena*, 2nd ed. (World Scientific, Singapore, 1992).
- [26] A. L. Barabasi and H. E. Stanley, *Fractal Concepts in Surface Growth* (Cambridge University Press, Cambridge, 1995).
- [27] S. Das Sarma and P. Tamborenea, *Phys. Rev. Lett.* **66**, 325 (1991).
- [28] P. I. Tamborenea and S. Das Sarma, *Phys. Rev. E* **48**, 2575 (1993).
- [29] S. Das Sarma, C. J. Lanczycki, S. V. Ghaisas, and J. M. Kim, *Phys. Rev. B* **49**, 10693 (1994).
- [30] J. L. Zubimendi, M. E. Vela, R. C. Salvarezza, L. Vazques, J. M. Vara, and A. J. Arvia, *Langmuir* **12**, 12 (1996).
- [31] S. O. Ferreira, I. R. B. Ribeiro, J. Suela, I. L. Menezes-Sobrinho, S. C. Ferreira, and S. G. Alves, *Appl. Phys. Lett.* **88**, 244102 (2006).
- [32] T. Ya'akov, M.Sc. thesis, Bar-Ilan University, Israel, 2006.